

Suprathermal electron beams and large sheath potentials generated by RF-antennas in the scrape-off layer of Tore Supra

J. P. Gunn 1), L. Colas 1), A. Ekedahl 1), E. Faudot 2), V. Fuchs 3), S. Heuraux 2), M. Goniche 1), M. Kočan 1), A. Mendes 1), A. Ngadjeu 2), V. Petržílka 3), F. Saint-Laurent 1), K. Vulliez 1)

1) CEA, IRFM, F-13108 St Paul-lez-Durance, France.

2) LPMIA, UMR 7040 CNRS, BP 239 F-54506 Vandoeuvre Cedex, France.

3) Assoc. EURATOM-IPP.CR, Za Slovankou 3, 182 21 Praha 8, Czech Republic

e-mail contact of main author: Jamie.Gunn@cea.fr

Abstract. In Tore Supra detailed radial-poloidal mapping of antenna-SOL interaction zones are made in a single shot using a retarding field analyzer (RFA) or Mach probe. A retarding field analyzer was used during LH current drive experiments to provide direct measurements of the particle and power fluxes of suprathermal electrons emanating from the region in front of the LH grill. When one of the active wave-guide rows is magnetically connected to the RFA, a strong particle flux due to suprathermal electrons is observed. A fraction of the electrons have energies greater than 1000 eV. Theory predicts that waves with high refractive index should be totally absorbed within at most 5 mm from the grill, and that the electron current should be stationary in time. In reality, electron current is measured at least 4-5 cm in front of the grill, and it exhibits a highly intermittent temporal evolution with a characteristic burst rate in the 10 kHz range. A Mach probe was used to map the SOL plasma parameters on flux tubes connected to both the standard and the new ITER-like ICRH antennae. A 1 cm layer of large positive floating potential (about one order of magnitude higher than the local electron temperature) is observed on flux tubes that graze the leading edges of the lateral protection limiters. Preliminary measurements of the true sheath potential using the RFA show that it is slightly more positive than the floating potential.

Introduction

In pursuit of its main mission to perform high power, steady state discharges, an impressive ensemble of safety systems based on real time feedback loops using a number of diagnostics is under continuous improvement in Tore Supra, a large tokamak ($R=2.4$, $a=0.72$, $B=4$ T, $I_p < 2$ MA) with a circular plasma defined by a bottom toroidal pump limiter (TPL). Highly reliable scenarios have been developed to allow detailed radial-poloidal mapping of the antenna-SOL interaction zones in a single shot using a retarding field analyzer (RFA) or Mach probe. Up to 15 reciprocations at a rate of 1 Hz have been made in a single full power discharge. Real time feedback on edge safety factor q_a is used to vary the magnetic connection between the probe and the antennas. The probe position itself is controlled by feedback on fast magnetic reconstruction to guarantee safe, reliable, and reproducible operation. Fast analysis of current-voltage characteristics and the instantaneous probe position provide input to a feedback routine that adapts the voltage of each electrode to the local SOL temperature, density, and floating potential, optimizing the dynamic range of the measurement.

According to theory Landau damping transfers the power carried by the high- $n_{//}$ spectrum components of the lower hybrid (LH) wave to thermal SOL electrons with energies of a few tens of eV and accelerates them up to a few keV [1]. In magnetic flux tubes passing just in front of the waveguides of LH antennae, a few percent of the launched LH wave power is absorbed by the scrape-off layer (SOL) plasma, transported long distances along field lines, and deposited on plasma-facing components. The power flux onto these "hot spots" is estimated to be several MW/m² by infra-red imagery in Tore Supra [2] and divertor plate thermocouples in TdeV [3], but no information concerning the current density or energy of

the particles can be obtained. Combined Langmuir and emissive probe measurements in front of a low power LH grill in the CASTOR tokamak demonstrated large sheath potentials in a thin layer, which, although indirect, could be consistent with the existence of suprathermal electrons [4].

2. Lower hybrid hot spots

A RFA [5] was used during LH current drive experiments to provide the first direct measurements of the particle and power fluxes of suprathermal electrons emanating from the region in front of the LH grills. The RFA is mounted on a vertically reciprocating probe drive, situated on top of the torus at $R=2.53$ m and toroidal angle $\phi=40^\circ$. The analyzer is biased to collect only suprathermal electrons with energy greater than 200 eV. The LH launcher (referred to as "C2") is in a horizontal port at $\phi=320^\circ$. The nominal radial position of the leading edge of its lateral protection limiter (LL) was $R_{C2}=3.138$ m at the midplane. A full mapping of the suprathermal electron current was measured by varying the plasma current from $I_p=0.72$ MA to 1.18 MA over 20 probe reciprocations on shots 39547, 39548, and 39551. The other main plasma parameters (major radius $R_0=2.38$ m, minor radius $a=0.72$ m, line-integrated density $\bar{n}_e = 3.5 \times 10^{19}$ m⁻², LH power $P_{C2}=1.5$ MW) were held constant. All four waveguide rows were active. A Langmuir probe in another vertical port at $\phi=160^\circ$ measured SOL profiles simultaneously on field lines that were not connected to the antenna. The SOL density was observed to be $5 \pm 1 \times 10^{17}$ m⁻³ at the antenna's radial position.

The mapping was calculated by integrating the field line equations in the positive toroidal direction from each point along the probe trajectory to the poloidal plane that intersects the left-hand edge of the grill as viewed from outside the tokamak [Fig. 1(a)]. At each point where the RFA measured electron current more negative than -100 μ A, a dot was placed on the map [Fig. 1(b)]. A hot spot is seen in front of each waveguide row. The leading edges of the hot spots describe an arc that has exactly the poloidal curvature of the LLs, but shifted radially inward by ~ 1.5 cm. The measurement of the launcher position lacks precision due to deformation of the flange under vacuum, dilation of the antenna under baking at 120°C , and hysteresis of the sliding contacts. A recent mechanical study of the system concluded that an uncertainty of

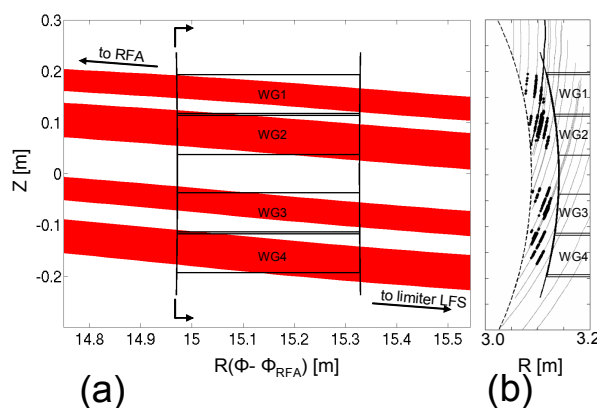


Fig. 1(a) LH antenna viewed from outside the machine looking inward along the major radius. Shaded regions indicate magnetic flux tubes in which suprathermal electrons are detected by the RFA. The four waveguide rows are labeled WG1 to WG4 from top to bottom. (b) Poloidal plane through the left hand edge of the antenna. The RFA trajectories mapped from the top of the machine are indicated by the thin gray curves, except for the sixteenth reciprocation (thick black curve) for which the raw data are displayed in Fig. 2. Black dots indicate positions at which electron current more negative than -200 μ A was detected. The dashed curve is the LCFS.

1 to 1.5 cm on the nominal launcher position is to be expected [6].

The suprathermal electron current measured on reciprocation #16 ($q_a=6.49$) is shown in Fig. 2. Zero collector current is measured when the RFA is behind the leading edge of the LL (gray shaded region in Fig. 3) indicating that the applied grid voltages are sufficient to fully repel all thermal ions and electrons. There is an abrupt transition to intense suprathermal electron current when the RFA begins to intercept field lines connected to the volume in front of WG1. The sharpness of the transition is consistent with the idea that the electrons are accelerated only on field lines that pass in front of the waveguides, and that they undergo no measurable radial spreading during their 15 m flight to the RFA. Near the grill the signal presents strong fluctuations superimposed upon a dc component. The electron current is sometimes strong enough to saturate the analog-to-digital convertors. The slit opening is $30\ \mu\text{m}$ wide by 5 mm long, therefore the flux density exceeds $5500\ \text{A}/\text{m}^2$. Multiplying by the RFA grid voltage, we find that the instantaneous peak power flux carried by the electrons is at least $(5500\ \text{A}/\text{m}^2)(200\ \text{V})=1.1\ \text{MW}/\text{m}^2$. The true value could be much higher because the electron energy is expected to be as high as a few keV according to theory.

Due to magnetic shear, the orientation of the mapped RFA trajectory in the R - Z plane is more poloidal than radial. After the first intense layer of electron current, a thin region is observed between WG1 and WG2 where again there is nearly zero signal. Then the RFA connects to the volume in front of WG2. Here, the RFA is already 1.5 cm radially in front of the grill. According to theory [7], within the first few millimetres, the high $n_{||}$ component of the LH wave should be fully absorbed by Landau damping on the cool SOL electrons. No electron acceleration should occur at these radial positions. It is thus remarkable that strong electron current is observed even at the deepest point of the reciprocation, 3.5 cm in front of the grill, at the LCFS.

The temporal character of the electron current varies radially. To qualify the nature of the signal we take a sample of measurements within a small radial range and calculate its mean \bar{I}_e and its most probable value I_e^{MP} . We equate I_e^{MP} with the dc component. When $\bar{I}_e \approx I_e^{MP}$, the electron current is defined to be “steady” (although fluctuating strongly around the mean). When the distribution of current is strongly skewed towards negative values such that $I_e^{MP}/\bar{I}_e \ll 1$ the signal is defined to be “bursty”. The characteristic repetition rate of the bursts is of the order of 10 kHz. It is interesting to note that this is consistent with the observed frequency range of natural SOL density fluctuations [8].

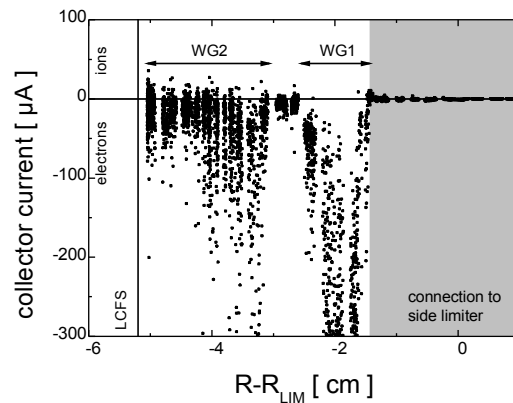


Fig. 2. Current measured by the collector versus midplane major radius relative to the leading edge of the LH antenna side limiter. Electron current is detected when the RFA is magnetically connected to waveguide rows WG1 or WG2 as indicated. The range of radial positions for which we believe the RFA to be connected to the side limiter of the LH antenna is coloured grey.

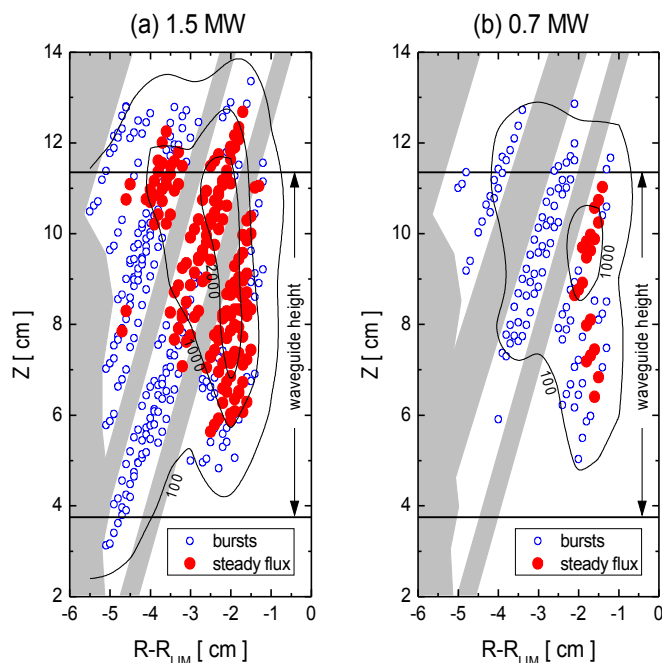


Fig. 3. Composite mapping of the flux of electrons with parallel energy greater than 200 eV for LH power (a) 1.5 MW and (b) 0.7 MW. Radial distance is measured with respect to the leading edge of the antenna's electron-side limiter. All data are shifted vertically to lie in front of the second waveguide row WG2. The horizontal black lines indicate the top and bottom walls of the waveguides. Areas where no data were measured are coloured grey. Full and open circles represent respectively points where the time-averaged electron current was more negative than $-50 \mu\text{A}$ or where 10% of the electron bursts were more negative than $-20 \mu\text{A}$. Approximate contours of time-averaged electron current density (A/m^2) are shown.

Bursts are observed even at the deepest points of the probe reciprocations on the LCFS, so we do not know how far in front of the LH grill they occur.

Interpolating the mean electron current density onto a regular grid and integrating over the composite hot spot we obtain 3.4 A, the total current of suprathermal electrons having parallel energy greater than 200 eV. This value underestimates the true value because the slit transmission coefficient is overestimated, the RFA did not go deep enough to fully map out the hot spots, and the electron current in the near field beam saturated the measuring circuit. Multiplying by 8 (assuming that the same current flows in both directions along the field lines from each of the 4 waveguide rows), we obtain a minimum estimate of the total LH power lost to the SOL electrons : $P_{\text{LOSS}} > 5.4 \text{ kW}$, or 0.35% of the total injected power. The true value could be several times higher, as explained above. Preliminary measurements of the full energy distribution at a fixed point in a hot spot have been carried out by varying U_{G2} down to -1000 V . These results will be presented in future work, but we can already report that despite visible attenuation of the electron flux at the most negative applied voltage, significant currents are still observed in both near field and far field beams, implying that a fraction of the electrons have energies greater than 1000 eV. Finally, it must be noted that the electrons

The measurements were shifted vertically to overlay the data and get a composite mapping of a single waveguide row with better spatial resolution [Fig. 3(a)]. Two principal regions are identified based on the temporal behaviour of the electron current. We refer to the layer of steady electron current adjacent to the leading edge of the LL as the "near field beam". It is defined to encompass all points where $\bar{I}_e < -50 \mu\text{A}$ (full circles on Fig. 3). The height of the layer is about the same as that of the waveguide rows (7.6 cm), but it is poloidally asymmetric, about 1 cm radial width across the bottom, and 3 to 4 cm across the top. Each hot spot is shifted upward $\sim 1 \text{ cm}$ with respect to the corresponding waveguide row, consistent with the tilt of the magnetic field lines [Fig. 1(a)]. Further away from the grill, we call the region of isolated intermittent bursts without a significant dc component the "far field beam". We define a point in space as belonging to the far field beam if 10% of the most negative current values are lower than $-20 \mu\text{A}$.

measured by the RFA are accelerated on field lines that pass in front of the LLs. There is additional power lost in the private flux region between the two limiters, adjacent to the grill mouth. The grill is about 1 to 3 mm behind the leading edges of the LLs, depending on the local toroidal field ripple for a given antenna position. Hot spots connected to each waveguide row are systematically recorded by infrared imagery. The power loss responsible for these hot spots was estimated to be in the range of 1% to 2% depending on plasma conditions [3]. We conclude that the power losses in the SOL are of similar magnitude as those in the private flux region of the grill.

The mapping was repeated with the antenna firing half as much power [Fig. 4(b)]. The SOL density only decreased by 10-20% on unconnected field lines. Both the near and far field beams are strongly reduced in size. The beam retains its poloidally asymmetric shape; the most intense current is displaced upwards with respect to the center of the profile for both power levels. The total current in the beam is 0.8 A, roughly four times less than for full power. The LH power loss fraction appears to have a strong non-linear dependence on the injected power. These measurements corroborate past findings [2].

These measurements suggest that theory needs to identify a mechanism, perhaps based on density fluctuations, for power transfer from the low- $n_{||}$ spectral peaks to high refractive indices at arbitrary distances from the grill. It has been known since the early 1980s that strong non-linear mechanisms such as the parametric decay instability with concomitant spectral broadening are at play near the LH antenna. If such a mechanism is indeed at work it could also resolve the persistent inability of present theory to explain the strong increase of localized SOL heating with density.

3. Flux tube biasing by ICRH antennas

The use of ICRH antennas has long been associated with the spurious generation of impurities in fusion devices. RF currents circulating in ICRH antenna straps, as well as those induced in the grounded antenna structure, create local electric fields that oscillate at the RF frequency. These electric fields act on the SOL plasma. Essentially, one considers individual magnetic field lines that pass in front of the antenna through regions of strong electric field [9], which is calculated using 3D electromagnetic codes [10]. If the parallel component of the electric field integrated along the magnetic field line is finite, then it is supposed that the potential drop across the sheaths connected to plasma-facing components should increase significantly above the value predicted by thermal sheath theory ($V_s - V_f \approx 3T_e$). This effect, known as RF sheath rectification, serves to maintain ambipolarity. The increased sheath potential should strongly accelerate incident ions, leading to enhanced sputtering from the surface. This is what causes the impurity production. If the antenna straps are appropriately phased, then the local electric fields should more or less compensate one another, minimizing sheath rectification. Due to the tilt of the field lines, however, diagonally opposite corners of the antenna are not compensated, and large sheath potentials are expected on field lines that are connected to those two regions, supposing that the 1D ambipolar sheath model can be applied separately to each magnetic field line.

A Mach probe at $\phi=160^\circ$ was used to map the SOL plasma parameters on flux tubes connected to both the standard and the new ITER-like ICRH antennas at $\phi=40^\circ$ on successive experimental campaigns. Previous measurements [11] were dedicated to flux tubes connected to the volume in front of the antenna straps. The poloidal distribution presented maxima near the top and bottom of the straps at $Z=\pm 0.3$ m, with a minimum near the antenna midplane.

Here we extend those measurements to the entire extension of the LL by running discharges with safety factor up to $q_a=9$ (Fig. 4). A 1 cm layer of large positive floating potential (about one order of magnitude higher than the local electron temperature) is observed on flux tubes that graze the leading edges of the LL. Even the shape of the upper tile corners can be distinguished, seen as a double peak on the probe trajectory that intercepts that region. It would thus appear that RF currents might also be generated in the LL, which have not yet been included in the 3D electromagnetic antenna codes (only the antenna box is modelled). The measurements are similar for both types of antenna. Combined uncertainties of the magnetic reconstruction, probe elevation, and the antenna's radial position prevent us from determining whether the biased flux tubes are connected to the LLs or if they pass in front of them. The total uncertainty, $\Delta R \sim 1-2$ cm, is comparable to the radial thickness of the biased layer. Large floating potentials are also observed on Langmuir probes at specific toroidal positions on the high-field side of the bottom toroidal limiter, in good correlation with the magnetic connection map. The perturbation induced by ICRH thus extends around the entire poloidal circumference of the SOL.

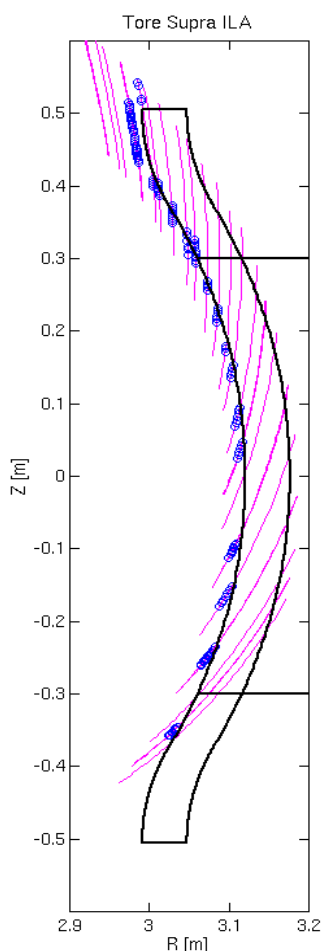


Fig. 4. Thin magenta lines are probe reciprocations mapped to the electron-side LL of the ITER-like antenna (the black curves show the profile of the LL and the horizontal lines at $Z=\pm 0.3$ m indicate the extent of the RF straps). Blue circles indicate floating potential greater than 20 V (peak values can reach 150 V) measured on the ion-side of the Mach probe, which is connected to the antenna.

These new measurements, as well as past ones in Tore Supra, all concern the floating potential measured by the ion-side of the Mach probe, which draws current from the low-field side of the tokamak, i.e. the side which looks towards the antennas. In contrast, the electron-side of the Mach probe, connected to the high-field side of the TPL, does not usually register large floating potentials, except when the probe is precisely connected to the lower edge of the antenna box at $Z=-0.3$ m as for example in shot 41869 (Fig. 5). The resolution of our poloidal mapping is insufficient to yield precise estimates of the size of this particular zone, but it is certainly no more than a few centimetres in poloidal extent. These measurements are perplexing: why would large floating potentials occur on the side of the probe that is not connected to the antenna in such a tiny region; while on the other hand, at the other positions, how should we interpret such a large difference between upstream and downstream floating potentials?

In order to compare with the model of antenna-SOL interaction, the sheath potential drop must be measured, not the floating potential, because it is the plasma potential at the entrance of the sheath that counts. The floating potential is nothing more than an indicator of non-ambipolarity (if the 1D model of sheath rectification were correct on individual field lines, then one would measure $V_f=0$ everywhere).

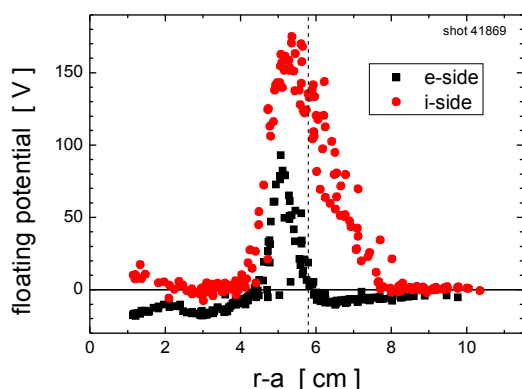


Fig. 5. Radial profiles of floating potential on the electron side of the Mach probe (not connected to the ICRH antenna) - squares - and the ion side (connected) -dots. These are raw data from 4 reciprocations into a single steady state discharge. The vertical dashed line indicates the leading edge of the LL.

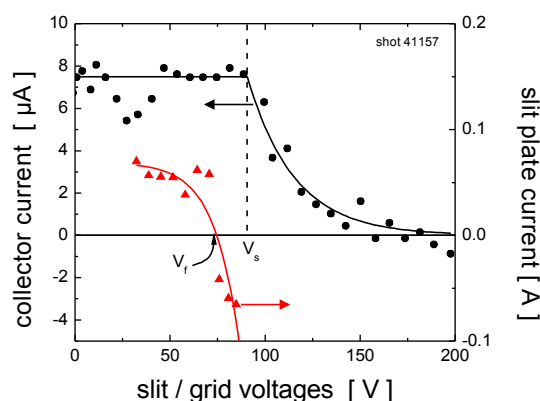


Fig. 6. RFA collector current vs. retarding grid voltage (dots). The voltage at which the current begins to decrease defines the sheath potential V_s . The local floating potential V_f is obtained from the I-V characteristic of the slit plate (triangles).

The true sheath potential V_s was recently measured by an emissive probe in Alcator-CMod [12]. In principle it can also be measured by the RFA. During the series of discharges shown in Fig. 4, the RFA was mounted on a second reciprocating probe drive located at $\varphi=40^\circ$, and was connected to a standard ICRH antenna at $\varphi=280^\circ$. Preliminary measurements of the sheath potential and floating potential profiles in the biased flux tube were measured simultaneously. The difference between the two should be of the order of the electron temperature according to thermal sheath theory, but unfortunately in this case the error bars are similar to that in magnitude (Fig. 6). The bias waveforms were not well adapted to measure these potentials precisely, but within experimental uncertainty, we can definitely conclude that the sheath potential is very similar to the floating potential or at best, slightly more positive. Dedicated measurements with suitable voltage resolution are needed.

It is interesting to note that the observation of local floating potentials more positive than vacuum vessel ground imply local nonambipolarity, i.e. net ion current flows from the connected flux tube into the tokamak wall. Thus, one of the assumptions of the 1D model is shown to be invalid. The polarity of the floating potential is difficult to understand. The radial gradient of plasma potential corresponds to a radial electric field directed from the center of the flux tube outward into the unperturbed SOL plasma. To be consistent with the observed net ion current to the wall, electron current would have to flow radially out of the flux tube to neighbouring flux surfaces, *against* the electric force (in violation of Ohm's law!), in order to maintain quasineutrality and satisfy current balance. Alternatively, if sheath rectification occurs in a small flux tube connected to a large grounded wall, then simple sheath theory, combined with dc electric current conservation, predicts that there should be net local electron current to the wall, i.e. the local dc floating potential should be negative rather than positive!

The polarity of the floating potential remains without theoretical explanation. The effect of long, positively biased flux tubes has been modelled, showing that ExB convection transports plasma radially and dumps it on the antenna structure, leading to enhanced heating and impurity release [13]. However, a self consistent model for the 3D potential including the

circulation of electric current including dc and rf effects has yet to be developed. The current loop has to be closed by net electron current to some other location in the tokamak (radial current to the antenna or another point on the tokamak wall? parallel current to the other end of the flux tube?). It would be helpful to make simultaneous probe measurements on both ends of a connected flux tube. For example, if charge balance is provided by parallel current flow, one would expect to find large negative floating potentials at the other end of the flux tube. Recent measurements in ASDEX [14] demonstrate that a net electron current flows to the ICRH antennas, while positive floating potentials are measured on connected field lines. This could occur if the antenna were positively biased rather than grounded.

Another aim of the RFA measurements was to determine whether any suprathermal particles are to be observed in the biased flux tube. No evidence of hot populations, neither ions nor electrons, was found.

With the proven reliability of its feedback systems, Tore Supra is in a unique position to perform detailed probe studies of RF-SOL interactions in view of high power operation in JET and in ITER. It is crucial to evaluate the density and power dependencies of heat flux due to LH electrons, and the consequences of the nonaxisymmetric 3D helical structure of ICRH-biased flux tubes on SOL transport. Future perspectives in Tore Supra include probe measurements during combined LH and ICRH operation to expand upon studies of antenna-antenna interaction based on infrared imagery [15].

Acknowledgements

The authors are greatly indebted to Jean-Yves Pascal for his untiring technical expertise. This work, supported by the European Communities under the contract of Association between EURATOM and CEA, was carried out within the framework of the European Fusion Development Agreement. The views and opinions expressed herein do not necessarily reflect those of the European Commission. Partly supported by the Czech Republic Grant Project GACR 202/07/0044.

References

- 1 V. Fuchs, et al., *Plasma Phys. Control. Fusion* **41** (1999) A495.
- 2 M. Goniche, et al., *Nuclear Fusion* **38** (1998) 919.
- 3 J. Mailloux, et al., *J. Nucl. Mater.* **241-243** (1997) 745.
- 4 F. Žáček, V. Petržílka, M. Goniche, *Plasma Phys. Contr. Fusion* **47**, L17 (2005).
- 5 M. Kočan, et al., *Rev. Sci. Instrum.* **79** (2008) 0735022.
- 6 E. Delmas, private communication (2007).
- 7 K. Rantamäki, et al., *Nuclear Fusion* **40** (2000) 1477.
- 8 P. C. Stangeby, "The plasma boundary of magnetic fusion devices," Institute of Physics Publishing, Bristol and Philadelphia, 369 (2000).
- 9 F. Perkins, *Nucl. Fusion* **29** (1989) 583.
- 10 L. Colas, et al., *Nucl. Fusion* **45** (2005) 767.
- 11 L. Colas, et al., *J. Nucl. Mater.* **363-365**, (2007) 555.
- 12 S. J. Wukitch, et al., 18th Conf. on Plasma Surface Interactions, Toledo, May 2008.
- 13 M. Bécoulet, et al., *Phys. Plasmas* **9** (2002) 2619.
- 14 V. Bobkov, et al., 18th Conf. on Plasma Surface Interactions, Toledo, May 2008.
- 15 L. Colas, et al., *Plasma Phys. Control. Fusion* **49** (2007) B35.